

# All-loop Mondrian Reduction of 4-particle Amplituhedron at Positive Infinity

---

Junjie Rao<sup>a\*</sup>

<sup>a</sup>*Max Planck Institute for Gravitational Physics (Albert Einstein Institute), 14476 Potsdam, Germany*

ABSTRACT: This article introduces a systematic framework to understand (not to derive yet) the all-loop 4-particle amplituhedron in planar  $\mathcal{N}=4$  SYM, utilizing both positivity and the Mondrian diagrammatics. Its key idea is the simplest one so far: we can decouple one or more sets of loop variables  $(x, y, z, w)$  from the rest by just setting these variables to either zero or infinity so that their relevant positivity conditions are trivialized, then the all-loop consistency requires that we get lower loop amplituhedra as “residues”. These decoupling relations connect higher loop DCI integrals with the lower ones, enabling us to identify their coefficients starting from the 3-loop case. And surprisingly, the delicate mechanism of this process is the simple Mondrian rule  $D=X+Y$ , which forces those visually non-Mondrian DCI integrals to have the correct coefficients such that the amplituhedron can exactly reduce to the lower loop one. Examples cover all DCI integrals at  $L=3, 4, 5, 6$ , especially, the subtle 6-loop coefficients  $+2$  and  $0$  are neatly explained in this way.

KEYWORDS: [Maximally supersymmetric scattering amplitudes](#), [Loop integrands](#), [Amplituhedron](#).

---

\*Email: [jrao@aei.mpg.de](mailto:jrao@aei.mpg.de)

---

## Contents

<b>1. Introduction</b>	<b>1</b>
<b>2. Nontrivialities at 4-loop</b>	<b>4</b>
<b>3. Rectangle and Block Removals at 5-loop</b>	<b>7</b>
<b>4. Identifications of the Rest Coefficients</b>	<b>8</b>
<b>5. Nontrivial Mondrian Diagrammatic Relations at 5-loop</b>	<b>11</b>
<b>6. Coefficients +2 and 0 at 6-loop</b>	<b>14</b>

---

## 1. Introduction

The amplituhedron proposal for 4-particle all-loop integrand of planar  $\mathcal{N}=4$  SYM [1, 2] is a novel reformulation which only uses positivity conditions for all physical poles to construct the integrand. At  $L$ -loop order, for any two sets of loop variables labelled by  $i, j=1, \dots, L$  we have the mutual positivity condition

$$D_{ij} = (x_j - x_i)(z_i - z_j) + (y_j - y_i)(w_i - w_j) > 0, \quad (1.1)$$

where positive variables  $x_i, y_i, z_i, w_i$  and  $D_{ij}$  are all possible physical poles. Though the dominating principle is simple and symmetric up to all loops, as the loop order increases, its calculational complexity grows explosively due to the highly nontrivial intertwining of all  $L(L-1)/2$  positivity conditions. Therefore it is more practical to seek new perspectives or techniques other than confronting the direct calculation, which however does not imply the direct calculation is impossible, as a better interpretation might redefine the problem so that the meaning of “direct” is more trivialized. This work shows how a simpler problem got complicated, then returns to its plain form after we switch to the correct perspective extracted from all the previous clues. So it is natural to expect the ultimate solution of 4-particle amplituhedron turns out to be even simpler, and hidden elegant patterns like the Mondrian story await to be discovered.

The most recent progress includes the direct calculation of the 3-loop case [3], the all-loop Mondrian diagrammatics [4] for a subset of dual conformally invariant (DCI) loop integrals of which pole structures can be Mondrianized, and the positive cuts [5] as a simplified approach to identify coefficients of a given basis of DCI integrals. This work continues to explore the 4-particle amplituhedron at higher loop orders,

as we will introduce a new systematic framework to more clearly integrate positivity with the Mondrian diagrammatics.

To begin to rebuild everything, forgetting all later advances, we can return to the original definition of this problem [1, 2]. First let's introduce a convenient convention for the following derivations: we will use the *dimensionless ratio* as the integrand, for example, in the 2-loop integral [2]

$$\int \frac{dx_1}{x_1} \frac{dy_1}{y_1} \frac{dz_1}{z_1} \frac{dw_1}{w_1} \frac{dx_2}{x_2} \frac{dy_2}{y_2} \frac{dz_2}{z_2} \frac{dw_2}{w_2} R \quad \text{where} \quad R = \frac{x_2 z_1 + x_1 z_2 + y_2 w_1 + y_1 w_2}{D_{12}}, \quad (1.2)$$

$R$  is the integrand we will extensively manipulate. In other words, the full integral is made up of the  $d \log$  measure of all positive variables and this ratio  $R$ . In particular, the 1-loop integrand is trivially 1 as there is no mutual positivity to be imposed. With this convention, when the integral is evaluated at either zero or infinity with respect to some variables, there is no extra factor to be added to the residual integrand, and the  $d \log$  measure of those unfixed variables can be dropped for convenience.

Then what use does this residue evaluation at zero or infinity have, which seems trivial compared to the positive cuts [5]? If we simply set  $x_j \rightarrow \infty$  and  $z_j = 0$  in

$$D_{ij} = (x_j - x_i)(z_i - z_j) + (y_j - y_i)(w_i - w_j) \rightarrow \infty z_i + (y_j - y_i)(w_i - w_j), \quad (1.3)$$

$D_{ij}$  becomes trivially positive, since the positivity of  $z_i$  is magnified by a positive infinity factor.

Let's be more concrete and immediately look at the 3-loop case:  $x_3 \rightarrow \infty$  and  $z_3 = 0$  lead to

$$D_{i3} \rightarrow \infty z_i + (y_3 - y_i)(w_i - w_3), \quad (1.4)$$

so  $D_{13}, D_{23}$  are positive, and we may claim that the third loop ‘‘decouples’’ from the rest two loops while positivity of  $D_{12}$  remains to be imposed. Now according to the integrands defined above (in terms of the 3-loop result given in [3]), namely

$$R_2 = \frac{x_2 z_1 + x_1 z_2 + y_2 w_1 + y_1 w_2}{D_{12}}, \quad (1.5)$$

$$R_3 = \frac{x_2 x_3 z_1 z_2 + y_2 y_3 w_1 w_2}{D_{12} D_{23}} + \frac{x_3^2 z_1 z_2 y_2 w_1 + x_2 x_3 z_1^2 y_3 w_2 + x_2 z_1 y_3^2 w_1 w_2 + x_3 z_2 y_2 y_3 w_1^2}{D_{12} D_{13} D_{23}} \quad (1.6)$$

+ (5 permutations of 1,2,3)

for  $L=2, 3$ , the residue of  $R_3$  at  $x_3 = \infty, z_3 = 0$  is exactly  $R_2$ ! This simple relation reflects the consistency of 4-particle amplituhedron as expected. We can further make it a bit more nontrivial by similarly setting  $y_3 = \infty, w_3 = 0$ , then

$$D_{i3} = \frac{1}{\varepsilon} (z_i + w_i), \quad (1.7)$$

where the infinitesimal  $\varepsilon$  is used to characterize the divergence of both  $x_3$  and  $y_3$ . Now the same relation  $R_3 \rightarrow R_2$  also holds but in a more interesting way as we will explain. Both situations above in fact encode the Mondrian diagrammatics [4]: in the first case a rectangle-like loop is removed, while in the second a

corner-like loop is removed, as visualized in figure 1. For the rectangle removal, as shown in the 1st line of figure 1, two examples of non-vanishing contributions are given, from which the reduction from  $R_3$  to  $R_2$  can be transparently seen. The non-vanishing criterion of a diagram is, its third loop must have contacts with the external faces  $y, z, w$  (here we keep using the convention in [3, 4, 5], namely faces  $x, z, y, w$  locate at the left, right, top and bottom of the diagram respectively). Similarly for the corner removal, a diagram must let its third loop have contacts with the external faces  $z, w$  in order to be non-vanishing. Of course, the rectangle or corner removal can have different choices of orientation by dihedral symmetry but without loss of generality, we stick to  $y, z, w$  or  $z, w$  for consistency as above.

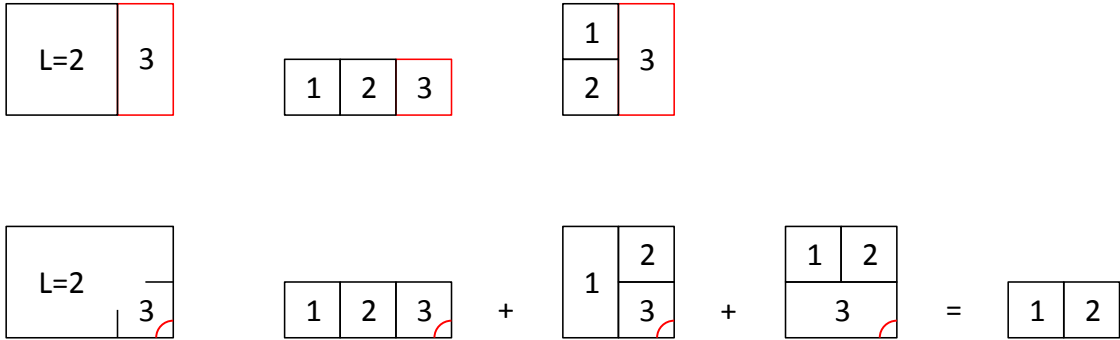


**Figure 1:** Rectangle removal and corner removal in Mondrian diagrammatics.

However, unlike the rectangle removal for which each 3-loop diagram simply reduces to a 2-loop one, the corner removal leads to more interesting relations among different 3-loop diagrams, as they together reduce to a 2-loop counterpart. As shown in the 2nd line of figure 1, after removing the third loop, these three diagrams reduce to the same 2-loop diagram but with various prefactors, of which the sum is unity:

$$\frac{z_2}{z_2 + w_2} + \frac{z_1}{z_1 + w_1} \frac{w_2}{z_2 + w_2} + \frac{w_1}{z_1 + w_1} \frac{w_2}{z_2 + w_2} = 1, \quad (1.8)$$

if we define

$$X_i = \frac{z_i}{z_i + w_i}, \quad Y_i = \frac{w_i}{z_i + w_i}, \quad D_i = X_i + Y_i = 1, \quad (1.9)$$

this is exactly the completeness relation in Mondrian diagrammatics [4]:

$$D_1 X_2 + X_1 Y_2 + Y_1 Y_2 = D_1 D_2. \quad (1.10)$$

Diagrammatically Mondrian factors  $X_i, Y_i, D_i$  mean loop 3 has a horizontal contact, vertical contact or no contact with loop  $i=1, 2$  respectively. From these easy examples of two types of loop removal, we see how the Mondrian diagrammatics helps understand the interconnections among different diagrams of various DCI topologies (including their coefficients) in an extremely neat way.

## 2. Nontrivialities at 4-loop

Next, we are curious to see how this wishfully simple mechanism deals with the more sophisticated 4-loop case, since it involves DCI topologies with coefficient  $-1$  and non-Mondrian pole structure, both of which are absent at lower loop orders. First of all, let's recall the 4-loop DCI topologies as given in figure 2.

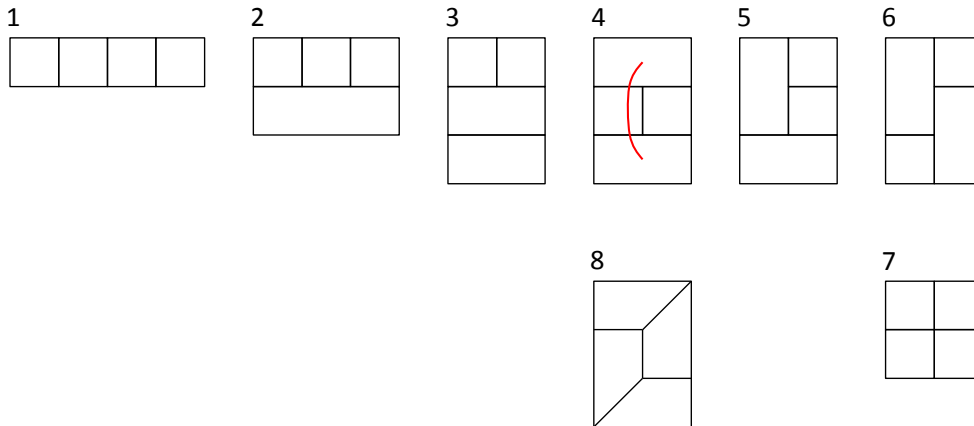


**Figure 2:** 4-loop DCI topologies (see [6]). The red curve denotes a rung rule factor  $D_{ij}$ , while rung rule factors  $x, y, z, w$  are diagrammatically suppressed for convenience.

Here topologies  $T_1, \dots, T_7$  are Mondrian while  $T_8$  is not. As we have known,  $T_7$  and  $T_8$  are associated with coefficient  $-1$ , and  $T_1, \dots, T_6$  are associated with  $+1$ , moreover,  $T_4$  has a  $D_{ij}$  factor in the numerator of its integrand. To see why these coefficients are so, we can pretend that they are still unknown yet and denote them by  $s_1, \dots, s_8$ . Immediately, we can perform the rectangle removal of loop 4. More rigorously speaking, we impose the limit

$$x_4 = \frac{1}{\varepsilon}, \quad z_4 = 0 \quad \text{where } \varepsilon \rightarrow 0 \quad (2.1)$$

in the 4-loop integrand  $R_4$ , which takes into account DCI loop integrals of all possible orientations given by dihedral symmetry (the number of which can be 8, 4, 2, or 1 for each topology) and all  $4!$  permutations of loop numbers. Then in the expansion

$$R_4(\varepsilon) = R_4(0) + O(\varepsilon), \quad (2.2)$$

the leading term  $R_4(0)$  depends on  $s_1, s_2, s_3, s_4, s_5$  only, and  $R_4(0) = R_3$  when  $s_1 = s_2 = s_3 = s_4 = s_5 = 1$  as expected. From the Mondrian diagrammatic perspective, this is trivial to understand as a 4-loop example of the rectangle removal. In fact we can further generalize the rectangle to remove more loops at a time, which will justify the existence of  $T_6, T_7$ . As visualized in figure 3, we now remove a block containing loop 3, 4 by imposing

$$x_3 = x_4 = \frac{1}{\varepsilon}, \quad z_3 = z_4 = y_3 = w_4 = 0, \quad (2.3)$$

so that for  $i=1,2$

$$D_{i3} = D_{i4} = \frac{1}{\varepsilon} z_i, \quad D_{34} = y_4 w_3, \quad (2.4)$$

note that  $\varepsilon$  helps regularize the expression  $(\infty - \infty)$  in  $D_{34}$  and renders this factor vanish. Then loop 3, 4 decouple from the rest two loops, and in the expansion

$$R_{4,2}(\varepsilon) = R_{4,2}(0) + O(\varepsilon) \quad (2.5)$$

where the additional subscript 2 of  $R_4$  denotes removing two loops at a time, we find

$$R_{4,2}(0) = \frac{s_3(x_2 z_1 + x_1 z_2) + (2s_6 + s_7)(y_2 w_1 + y_1 w_2)}{D_{12}}, \quad (2.6)$$

which equals  $R_2$  when  $s_3 = s_6 = 1$  and  $s_7 = -1$ . This is also easy to understand diagrammatically, and the interesting combination  $(2s_6 + s_7)$  explains why we need a minus sign for the cross topology  $T_7$ : the block removal of loop 3, 4 of two different orientations of  $T_6$  gives the same 2-loop diagram, therefore one must be eliminated in order to maintain  $R_{4,2}(0) = R_2$  while all orientations of  $T_6$  and  $T_7$  are used exactly once, as shown in figure 3. This cancelation mechanism is somehow analogous to the cancelation between the cross and the brick-wall patterns in Mondrian diagrammatics [4], and we will see more examples at higher loop orders.

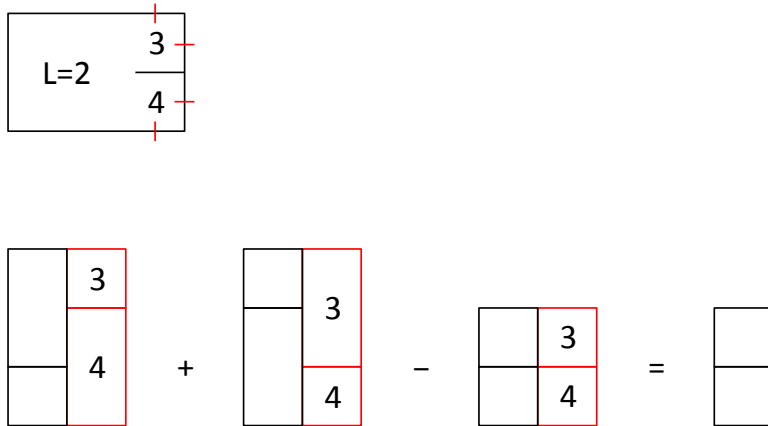


**Figure 3:** Block removal and the cancelation between  $T_6$  and  $T_7$  in  $R_4 \rightarrow R_2$ .

Now only  $s_8$  awaits to be explained and we must use the corner removal to detect this non-Mondrian topology  $T_8$ , since it has no rectangle or block to be properly removed. Similarly, for removing loop 4 we impose the limit

$$x_4 = y_4 = \frac{1}{\varepsilon}, \quad z_4 = w_4 = 0, \quad (2.7)$$

then in the expansion  $R_4(\varepsilon) = R_4(0) + O(\varepsilon)$ , we find

$$R_4(0) - R_3 \propto 1 + s_8, \quad (2.8)$$

to maintain the consistency we must take  $s_8 = -1$ . This is easy to understand if we look at  $T_4, T_8$  together among others, as the  $D_{ij}$  factor in the numerator of  $T_4$ 's integrand requires a counter term for producing the correct Mondrian factor. More concretely, in the 1st line of figure 4 the relevant two diagrams give

$$\frac{x_2 x_3 x_4 z_1 z_2 z_3 y_3 w_2}{D_{12} D_{13} D_{23} D_{24} D_{34}} (D_{14} - y_4 w_1) = \frac{z_2}{z_2 + w_2} \frac{z_3}{z_3 + w_3} \times \frac{x_2 x_3 z_1^2 y_3 w_2}{D_{12} D_{13} D_{23}} + O(\varepsilon) \quad (2.9)$$

after using

$$D_{14} - y_4 w_1 = \frac{1}{\varepsilon} (z_1 + w_1) - \frac{1}{\varepsilon} w_1 = \frac{1}{\varepsilon} z_1, \quad (2.10)$$

where

$$\frac{z_2}{z_2 + w_2} \frac{z_3}{z_3 + w_3} = X_2 X_3 \quad (2.11)$$

is the desired Mondrian factor, which characterizes the contacting relation between loop 4 in the diagram of topology  $T_4$  and the 3-loop sub-diagram (or the resulting 3-loop diagram at the RHS).

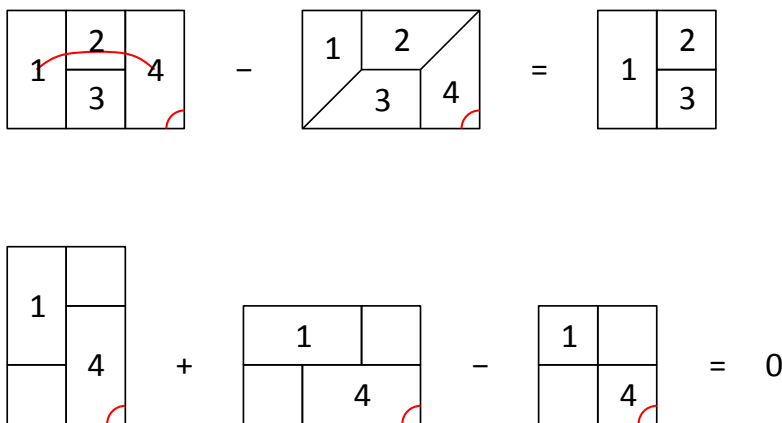


**Figure 4:** New features of the 4-loop corner removal.

Moreover, the cancelation between  $T_6$  and  $T_7$  in the 4-loop corner removal  $R_4 \rightarrow R_3$  again holds, as the relevant three diagrams in the 2nd line of figure 4 lead to the combination

$$x_4 z_1 + y_4 w_1 - D_{14} = \frac{1}{\varepsilon} z_1 + \frac{1}{\varepsilon} w_1 - \frac{1}{\varepsilon} (z_1 + w_1) = 0, \quad (2.12)$$

which is exactly isomorphic to the cancelation between the cross and the brick-wall patterns in Mondrian diagrammatics [4].

Let's summarize the nontrivialities in the 4-loop case via understanding  $s_1, \dots, s_8$ . First, it is useful to generalize the rectangle removal to the block removal, in order to check the consistency of decoupling more than one loop at a time. At 6-loop order we will also need the block removal of three loops, and so on. Next, topologies  $T_7, T_8$  with coefficient  $-1$  serve as counter terms of those with  $+1$ , and while  $T_7$  has a clear meaning in Mondrian diagrammatics,  $T_8$  appears to be the necessary company of  $T_4$  which has a

nontrivial  $D_{ij}$  factor in its integrand. At 5-loop order and higher, even a company topology or a group of company topologies will have its further company, enriching the diversity of contributing topologies while maintaining the overall Mondrian consistency.

### 3. Rectangle and Block Removals at 5-loop

To see more nontrivial examples of various patterns found at  $L=3, 4$ , and to check whether new features or exceptions appear, we move on to the 5-loop case. First let's recall the 5-loop DCI topologies as given in figure 5, where all 34 topologies are reorganized for later convenience while the same labels used in [5] are kept.

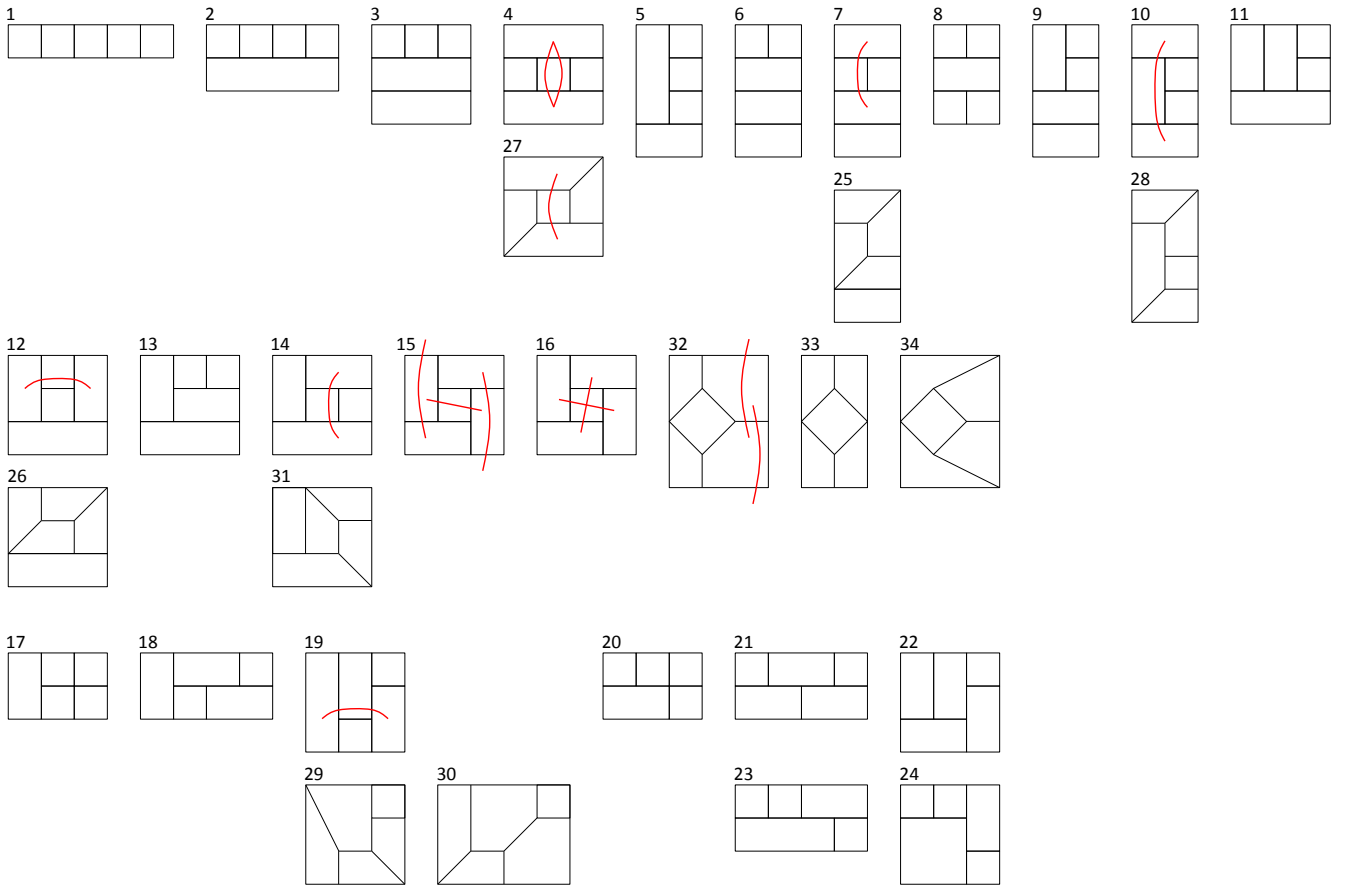


**Figure 5:** 5-loop DCI topologies (see [7]). The red curves denote  $D_{ij}$  factors, while  $x, y, z, w$  factors for  $T_{15}$  and  $T_{32}$  are also indicated for clarity.

Note that according to the classification in [4],  $T_1, \dots, T_{14}$  are of the ladder type and  $T_{17}, \dots, T_{24}$  are of the cross and brick-wall types. The coefficients or signs of these topologies can be immediately determined



by the rule that each cross pattern contributes  $-1$  multiplicatively (otherwise 1), explicitly we have

$$s_1 = s_2 = s_3 = s_4 = s_5 = s_6 = s_7 = s_8 = s_9 = s_{10} = s_{11} = s_{12} = s_{13} = s_{14} = 1, \quad (3.1)$$

$$s_{17} = s_{20} = -1, \quad s_{18} = s_{19} = s_{21} = s_{22} = s_{23} = s_{24} = 1. \quad (3.2)$$

Additionally, each of  $T_{25}, T_{26}$  has an obvious attached rectangle, therefore their signs automatically follow that of  $T_8$  in the 4-loop case, namely  $s_{25} = s_{26} = -1$ .

Upon these inputs, we find the rectangle removal of loop 5

$$x_5 = \frac{1}{\varepsilon}, \quad z_5 = 0 \quad (3.3)$$

leads to  $R_5(0) = R_4$  as expected. And the block removal of loop 4, 5

$$x_4 = x_5 = \frac{1}{\varepsilon}, \quad z_4 = z_5 = y_4 = w_5 = 0 \quad (3.4)$$

leads to

$$R_{5,2}(0) - R_3 \propto 2s_{15} + s_{16} + 2s_{32} + s_{33}, \quad (3.5)$$

which should be zero as required by the consistency. To confirm this guess and to further fully understand the 5-loop case, let's identify  $s_{15}, s_{16}$  and  $s_{27}, \dots, s_{34}$  one by one, similar to the identification of  $s_8$  in the 4-loop case.

#### 4. Identifications of the Rest Coefficients

First of all,  $s_{28}, s_{29}, s_{30}$  can be trivially determined by the 4-loop knowledge. Obviously,  $T_{28}$  is the company topology of  $T_{10}$ , similar to the fact that  $T_8$  is the company topology of  $T_4$  in the 4-loop case, as the  $T_{10}, T_{28}$  pair is the counterpart of the  $T_4, T_8$  pair plus one rung. Similarly,  $T_{29}, T_{30}$  are the company topologies of  $T_{19}$ , note that  $T_{29}$  has one rung rule factor and  $T_{30}$  has two substitution rule factors which result from the corresponding rung rule factor of  $T_{19}$ . Therefore we simply have  $s_{28} = s_{29} = s_{30} = -1$ .

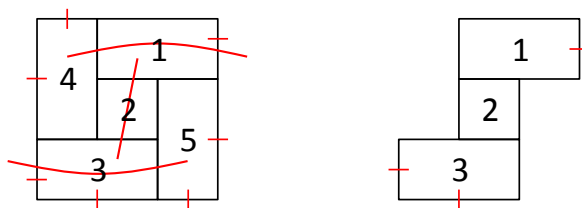


**Figure 6:** Identification of  $s_{15}, s_{16}$ : removing loop 4,5 with additional cuts on loop 1,3.

Now let's consider  $s_{15}, s_{16}$  which are a bit tricky. To separate  $s_{15}, s_{16}$  from other unknown coefficients, we impose as many cuts as possible around the rim of a particular  $T_{15}$  diagram, as shown in figure 6, and

then use a special two-step expansion. To disentangle  $s_{15}$  and  $s_{16}$ , we also relax one external cut, namely  $y_1$  here, and the reason to do so will be clear shortly. Explicitly, we impose the limit

$$x_5 = z_4 = \frac{1}{\varepsilon_1}, \quad y_5 = w_4 = \frac{1}{\varepsilon_2}, \quad y_4 = x_4 = x_3 = w_3 = w_5 = z_5 = z_1 = 0, \quad (4.1)$$

then in the two-step expansion (note the order of expansions matters as we intentionally utilize the  $x_5, z_4$  factors of this diagram to separate it from other sub-leading contributions)

$$R'_5(\varepsilon_1, \varepsilon_2) = R'_5(0, \varepsilon_2) + O(\varepsilon_1), \quad R'_5(0, \varepsilon_2) = R'_5(0, 0) + O(\varepsilon_2), \quad (4.2)$$

where the prime denotes additional cuts  $x_3 = w_3 = z_1 = 0$  besides removing loop 4,5 as indicated in figure 6, we find

$$R'_5(0, 0) - R'_3 \propto (s_{15} + s_{16}) y_1 w_1 - (2 s_{15} + s_{16} - 1) y_3 w_1 - (2 s_{15} + s_{16} + 2 s_{32} + s_{33}) x_1 z_3. \quad (4.3)$$

To maintain the consistency we must have  $s_{15} + s_{16} = 0$  and  $2s_{15} + s_{16} = 1$ , so  $s_{15} = 1$  and  $s_{16} = -1$ , which explains why  $y_1$  must be non-vanishing, otherwise we cannot identify  $s_{15}, s_{16}$  with merely  $2s_{15} + s_{16} = 1$ . As we have assumed  $2s_{15} + s_{16} + 2s_{32} + s_{33} = 0$  in the previous section, this condition reduces to  $2s_{32} + s_{33} = -1$  which awaits to be confirmed.

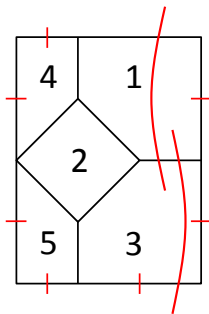


**Figure 7:** Identification of  $s_{31}, s_{32}, s_{33}$ : removing loop 4,5 with additional cuts on loop 1,3.

Next, we can identify  $s_{31}, s_{32}, s_{33}$  upon the inputs of  $s_{15}, s_{16}, s_{30}$  in a similar way. Picking a particular  $T_{32}$  diagram as given in figure 7, we impose the limit

$$z_4 = w_4 = z_5 = y_5 = \frac{1}{\varepsilon}, \quad y_4 = x_4 = x_5 = w_5 = w_3 = z_3 = z_1 = 0, \quad (4.4)$$

and note the external cut of  $y_1$  is relaxed, then in the expansion  $R'_5(\varepsilon) = R'_5(0) + O(\varepsilon)$  we find

$$R'_5(0) - R'_3 \propto (1 + s_{31}) x_2 x_3 y_1 + (s_{32} + s_{33}) x_2 y_1 (x_3 - w_1) + (1 + 2 s_{32} + s_{33}) x_2 (x_1 x_3 + y_3 w_1), \quad (4.5)$$

so the consistency requires  $s_{31} = s_{32} = -1$  and  $s_{33} = 1$ . Again,  $y_1$  must be non-vanishing, otherwise we can merely know one condition. Now we have confirmed  $2s_{32} + s_{33} = -1$  and hence  $2s_{15} + s_{16} + 2s_{32} + s_{33} = 0$ .

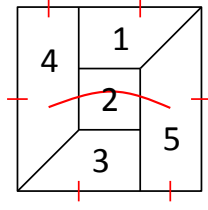


**Figure 8:** Identification of  $s_{27}$ : removing loop 4,5 with additional cuts on loop 1,3.

Then for  $s_{27}$ , we can pick a particular  $T_{27}$  diagram as given in figure 8 and impose the limit

$$z_4 = w_4 = x_5 = y_5 = \frac{1}{\varepsilon}, \quad y_1 = y_4 = x_4 = w_3 = w_5 = z_5 = 0, \quad (4.6)$$

now upon the inputs of  $s_{15}, s_{16}$  and  $s_{28}, \dots, s_{33}$ , we find

$$R'_5(0) - R'_3 \propto 1 + s_{27}, \quad (4.7)$$

therefore  $s_{27} = -1$ .

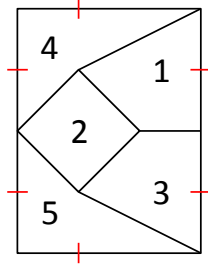


**Figure 9:** Identification of  $s_{34}$ : removing loop 4,5 with additional cuts on loop 1,3.

Finally for  $s_{34}$ , we can pick a particular  $T_{34}$  diagram as given in figure 9 and impose the limit

$$z_4 = w_4 = z_5 = y_5 = \frac{1}{\varepsilon}, \quad y_4 = x_4 = x_5 = w_5 = z_3 = z_1 = 0, \quad (4.8)$$

upon the inputs of  $s_{15}, s_{16}$  and  $s_{30}, \dots, s_{33}$  we find

$$R'_5(0) - R'_3 \propto s_{34} - 1, \quad (4.9)$$

therefore  $s_{34} = 1$ . In summary, in this section we have proved that

$$s_{15} = 1, \quad s_{16} = -1, \quad s_{27} = s_{28} = s_{29} = s_{30} = s_{31} = s_{32} = -1, \quad s_{33} = s_{34} = 1, \quad (4.10)$$

together with the previous section, all 34 coefficients of 5-loop DCI topologies are now identified.

## 5. Nontrivial Mondrian Diagrammatic Relations at 5-loop

Knowing all these coefficients, we then proceed further to understand them, for example, why a coefficient is  $-1$  instead of  $1$ , which should not be just an incidental result of imposing cuts at either zero or infinity. Once we find the Mondrian interconnections among various DCI topologies, their coefficients will become a natural consequence of the simple relations extracted from previous derivations.

More concretely, we would like to explain the universal decoupling relation using one corner removal, which, unlike the rectangle or block removal, can cover all topologies. The limit to be imposed is simple:

$$x_5 = y_5 = \frac{1}{\varepsilon}, \quad z_5 = w_5 = 0, \quad (5.1)$$

namely removing loop 5, then in the expansion  $R_5(\varepsilon) = R_5(0) + O(\varepsilon)$  we find  $R_5(0) = R_4$ . However, this is not the end of the story since  $R_5(0) = R_4$  is a redundant relation and it can be further dissected into many much more transparent sub-relations, as diagrammatically shown in figures 10 and 11.

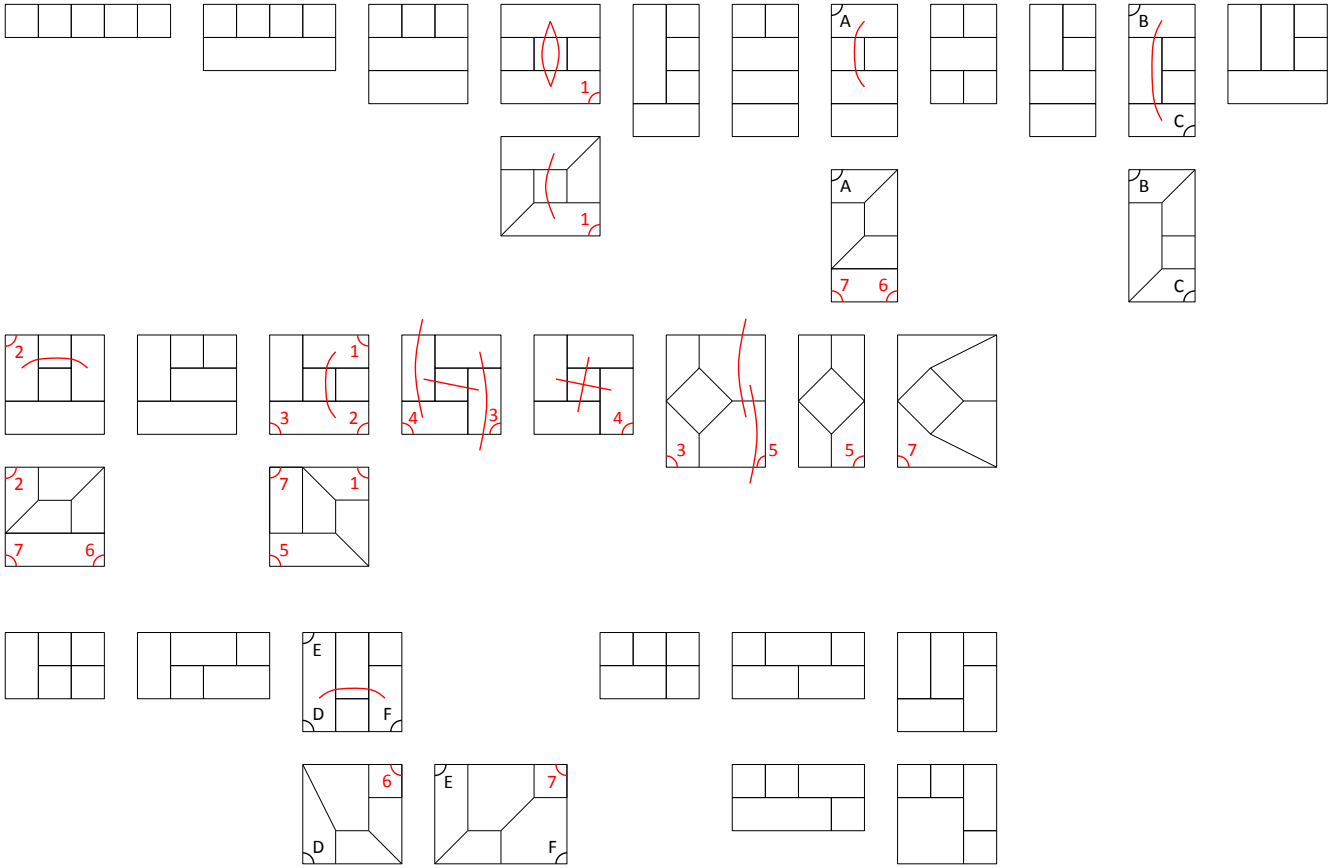


**Figure 10:** Nontrivial corners of 5-loop DCI topologies. Groups  $A, \dots, F$  in black denote relations that are direct extensions of the 4-loop case. Groups  $1, \dots, 7$  in red denote new relations at 5-loop.

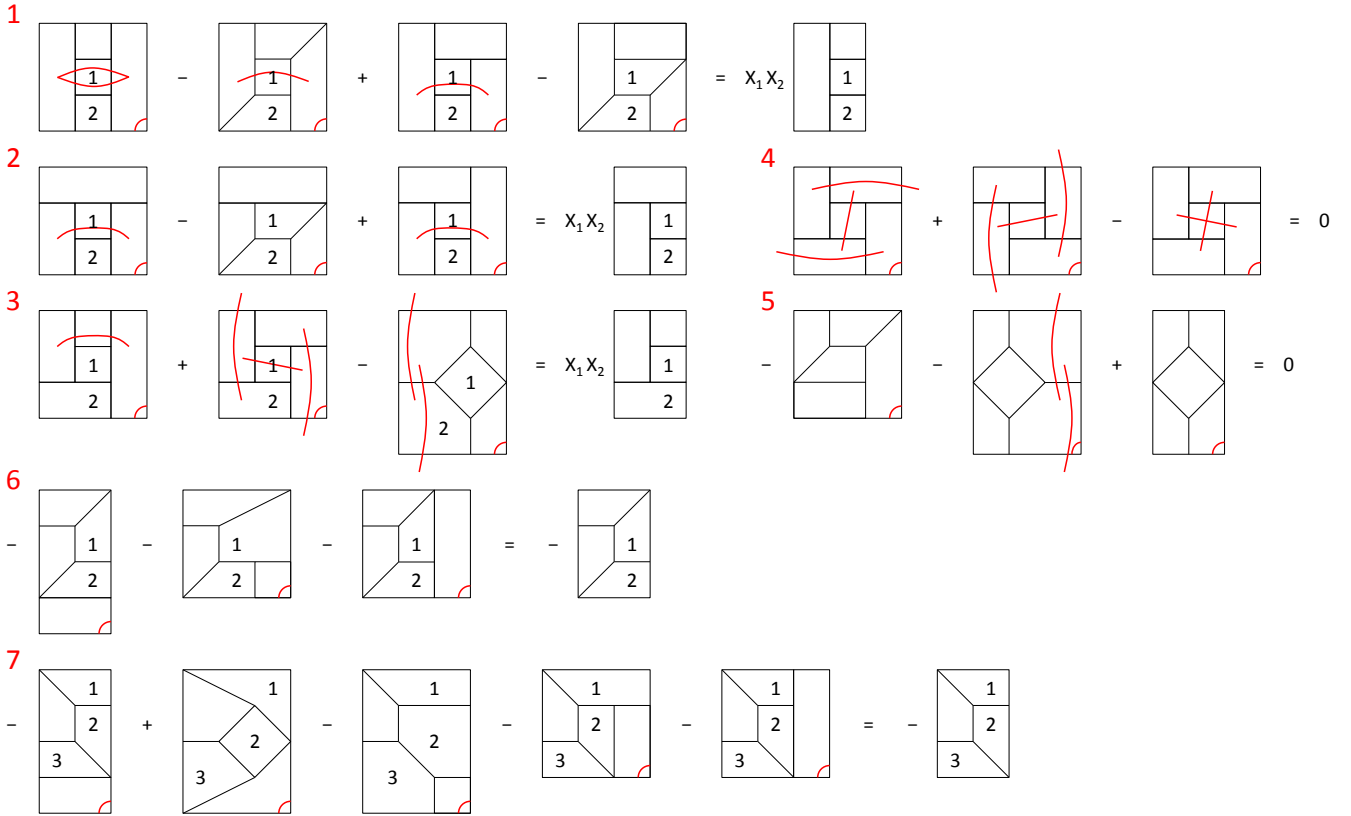


**Figure 11:** New Mondrian diagrammatic relations at 5-loop: groups 1, 2, 3 are the relations with obvious Mondrian pole structures, groups 4, 5 are the vanishing or canceling relations and groups 6, 7 are the relations of non-Mondrian company topologies.

In figure 10, all nontrivial corner removals of 5-loop DCI topologies are indicated. We will focus on groups of corners denoted by  $1, \dots, 7$ , while groups denoted by  $A, \dots, F$  are the direct extensions of the corner removals of  $T_4, T_8$  in the 4-loop case (see figure 4). The rest unmentioned corners are as trivial as the 3-loop corners or 4-loop corners except those of  $T_4, T_8$ , as they locate in visually Mondrian topologies and do not involve the  $D_{ij}$  factor.

In figure 11, groups  $1, \dots, 7$  are further separated into three types so that we can more clearly understand their nontrivialities, let's select one example from each type to elaborate these delicate relations. In the 1st diagrammatic equality, the 1st and 3rd diagrams have Mondrian pole structures, and in these two diagrams the removed loop has horizontal contacts with loop 1, 2 while its contact with the unlabeled loop on top of loop 1 is horizontal in the 1st diagram and vertical in the 3rd. Naively this should give

$$X_1 X_2 X_3 + X_1 X_2 Y_3 = X_1 X_2 D_3 = X_1 X_2 \tag{5.2}$$

according to the definitions in (1.9), which uses a Mondrian completeness relation and here 3 denotes the

unlabeled loop. However, the  $D_{ij}$  factors in the 1st and 3rd diagrams complicate this relation and that's why we also need the 2nd and 4th diagrams with minus signs to offset that, then we can exactly get the neat result at the RHS with Mondrian factor  $X_1X_2$ . The 2nd and 3rd diagrammatic equalities share the same feature of needing non-Mondrian company topologies, to offset the extra complexity brought by the  $D_{ij}$  factors. However, such a company topology does not have one-to-one correspondence to a particular Mondrian topology, unlike the  $T_4, T_8$  pair at 4-loop.

For the 4th diagrammatic equality, under the corner removal, schematically it is proportional to  $X + Y - D$ , so it simply vanishes. The 5th equality follows exactly the same cancelation mechanism, though it is not so obvious as the 4th.

For the 6th diagrammatic equality, under the corner removal three non-Mondrian diagrams sum to a 4-loop non-Mondrian diagram, due to

$$D_1Y_2 + Y_1X_2 + X_1X_2 = D_1D_2 = 1. \quad (5.3)$$

Though the resulting 4-loop diagram is not Mondrian, its contact with the 5th loop is still Mondrian, so that we can use the Mondrian completeness relation. The 7th equality is similar but more nontrivial as

$$D_1D_2Y_3 - D_1X_2Y_3 + D_1Y_2X_3 + Y_1X_2D_3 + X_1X_2D_3 = D_1D_2D_3 = 1, \quad (5.4)$$

note the 2nd diagram has a plus sign so it contributes a minus in the Mondrian completeness relation, as the resulting 4-loop diagram also has a minus sign. The Mondrian factor  $D_1X_2Y_3$  from this diagram is not obvious in the sense of horizontal and vertical contacts, but we can deform its external profile to manifest this, as shown in figure 12. Now the external profile of this 5-loop diagram is not a rectangle, but we can see a familiar 4-loop non-Mondrian diagram hidden in it. With Mondrian factor  $D_1X_2Y_3$  clarified, which is the desired result for offsetting two  $D_1X_2Y_3$  factors from the rest four diagrams, we see the Mondrian diagrammatics works more effectively than naive visual intuition. A final remark is, the 2nd diagram also serves as a company topology of the rest four, similar to the complexity of the first three identities.

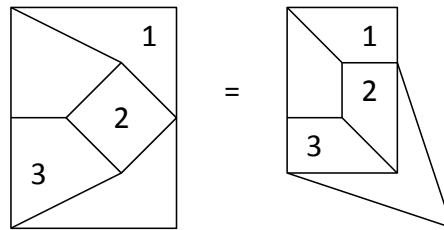


**Figure 12:** Deformation to manifest Mondrian factor  $D_1X_2Y_3$ .

## 6. Coefficients +2 and 0 at 6-loop

Finally we can take a glance at the 6-loop case, by investigating the coefficients of two special 6-loop DCI topologies. First of all, the 6-loop amplituhedron or integrand involves 229 non-vanishing contributions of DCI topologies, among which 125 have Mondrian pole structures as listed in Appendix B of [4], while the rest 104 non-Mondrian ones are the company topologies in the sense of corner removal. Interestingly, we also need six vanishing DCI topologies, namely those with coefficient 0, for a complete understanding of the 6-loop corner removal. All these topologies with coefficients can be found in the original result [8].

Similar to the 5-loop case we have extensively described, the new Mondrian diagrammatic relations at 6-loop also can be separated into three types: those with obvious Mondrian pole structures, the vanishing or canceling ones and those of non-Mondrian company topologies. Now we consider two particular 6-loop DCI topologies with three relevant Mondrian diagrammatic relations, as shown in figure 13.

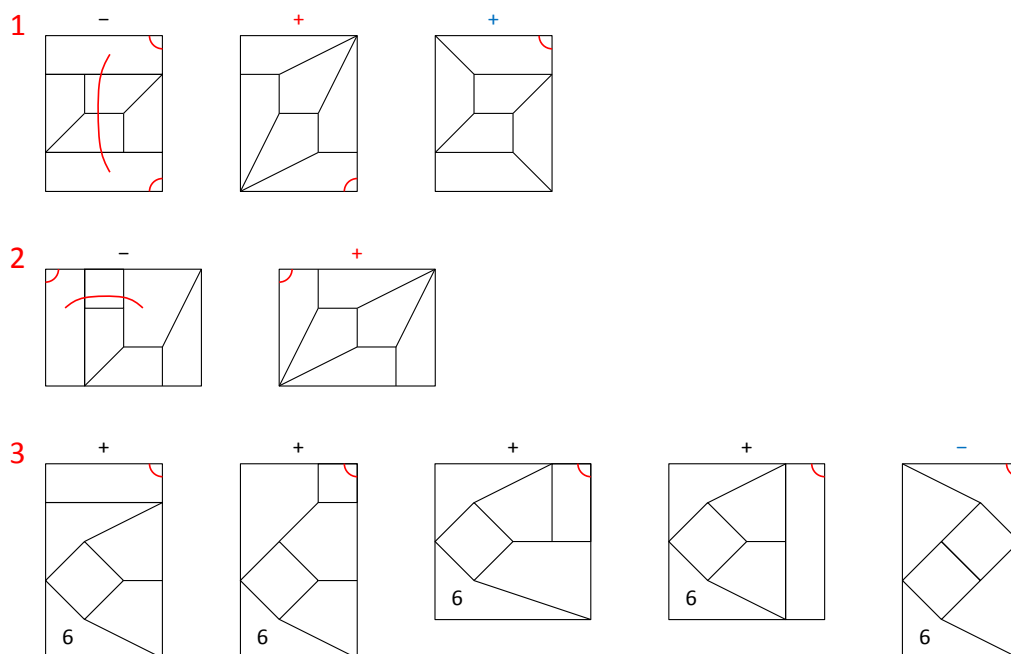


**Figure 13:** The two plus signs in red of the first topology add up to +2, while the plus and minus signs in blue of the second topology add up to 0, in three relevant Mondrian diagrammatic relations.

The first topology is the 2nd diagram in the 1st relation, or the 2nd diagram in the 2nd relation, as each of them serves as a company topology of the 1st diagram in the 1st or 2nd relation, following exactly the same mechanism of  $T_4, T_8$  pair at 4-loop (see figure 4). Since this topology appears twice and in both situations it has a plus sign, its overall coefficient is simply +2 as we add up these two pluses!

Similarly, the second topology is the 3rd diagram in the 1st relation, as a company topology for the other corner of the 1st diagram, or the 5th diagram in the 3rd relation, and note that they belong to the

same topology though drawn differently. Now in both situations it has a plus and a minus, so these two signs cancel and its overall coefficient is 0! One may find the 3rd relation unfamiliar, but it is simply the 7th relation in figure 11 if we remove the 6th loop as indicated in figure 13. Imagine the deformation in figure 12 to better visualize this analogy, one will find this 6-loop relation completely trivial based on its 5-loop counterpart with an overall sign reverse for all topologies. Then the two special coefficients +2 and 0 are neatly explained.

At 7-loop order there is no novelty other than +2 and 0 coefficients [8], while starting from the 8-loop case fractional coefficients begin to appear [9, 10]. Therefore we expect a nontrivial generalization of the Mondrian diagrammatic relations at  $L \geq 8$ , but they should be not too exotic since these coefficients are still rational. Finally, we would like to explore how the Mondrian consistency connecting amplituhedra of different loop orders can be extended to the generic case of more than four particles [11, 12, 13], or what it can tell us about the latter from the 4-loop knowledge [14].

## References

- [1] N. Arkani-Hamed and J. Trnka, “The Amplituhedron,” *JHEP* **1410**, 030 (2014) [arXiv:1312.2007 [hep-th]].
- [2] N. Arkani-Hamed and J. Trnka, “Into the Amplituhedron,” *JHEP* **1412**, 182 (2014) [arXiv:1312.7878 [hep-th]].
- [3] J. Rao, “4-particle Amplituhedron at 3-loop and its Mondrian Diagrammatic Implication,” *JHEP* **1806**, 038 (2018) [arXiv:1712.09990 [hep-th]].
- [4] Y. An, Y. Li, Z. Li and J. Rao, “All-loop Mondrian Diagrammatics and 4-particle Amplituhedron,” *JHEP* **1806**, 023 (2018) [arXiv:1712.09994 [hep-th]].
- [5] J. Rao, “4-particle Amplituhedronics for 3-5 loops,” *Nucl. Phys. B* **943**, 114625 (2019) [arXiv:1806.01765 [hep-th]].
- [6] Z. Bern, M. Czakon, L. J. Dixon, D. A. Kosower and V. A. Smirnov, “The Four-Loop Planar Amplitude and Cusp Anomalous Dimension in Maximally Supersymmetric Yang-Mills Theory,” *Phys. Rev. D* **75**, 085010 (2007) [hep-th/0610248].
- [7] Z. Bern, J. J. M. Carrasco, H. Johansson and D. A. Kosower, “Maximally supersymmetric planar Yang-Mills amplitudes at five loops,” *Phys. Rev. D* **76**, 125020 (2007) [arXiv:0705.1864 [hep-th]].
- [8] J. L. Bourjaily, A. DiRe, A. Shaikh, M. Spradlin and A. Volovich, “The Soft-Collinear Bootstrap: N=4 Yang-Mills Amplitudes at Six and Seven Loops,” *JHEP* **1203**, 032 (2012) [arXiv:1112.6432 [hep-th]].
- [9] J. L. Bourjaily, P. Heslop and V. V. Tran, “Perturbation Theory at Eight Loops: Novel Structures and the Breakdown of Manifest Conformality in N=4 Supersymmetric Yang-Mills Theory,” *Phys. Rev. Lett.* **116**, no. 19, 191602 (2016) [arXiv:1512.07912 [hep-th]].
- [10] J. L. Bourjaily, P. Heslop and V. V. Tran, “Amplitudes and Correlators to Ten Loops Using Simple, Graphical Bootstraps,” *JHEP* **1611**, 125 (2016) [arXiv:1609.00007 [hep-th]].
- [11] N. Arkani-Hamed, H. Thomas and J. Trnka, “Unwinding the Amplituhedron in Binary,” *JHEP* **1801**, 016 (2018) [arXiv:1704.05069 [hep-th]].



- [12] N. Arkani-Hamed, C. Langer, A. Yelleshpur Srikant and J. Trnka, “Deep Into the Amplituhedron: Amplitude Singularities at All Loops and Legs,” *Phys. Rev. Lett.* **122**, no. 5, 051601 (2019) [arXiv:1810.08208 [hep-th]].
- [13] R. Kojima, “Triangulation of 2-loop MHV Amplituhedron from Sign Flips,” *JHEP* **1904**, 085 (2019) [arXiv:1812.01822 [hep-th]].
- [14] P. Heslop and V. V. Tran, “Multi-particle amplitudes from the four-point correlator in planar  $\mathcal{N} = 4$  SYM,” *JHEP* **1807**, 068 (2018) [arXiv:1803.11491 [hep-th]].